

Electron-Transfer Component in Hydroxyl Radical Reactions Observed by Time Resolved Resonance Raman Spectroscopy[†]

G. N. R. Tripathi

Contribution from the Radiation Laboratory, University of Notre Dame, Notre Dame, Indiana 46556

Received January 6, 1998

Abstract: The existence of an electron-transfer pathway in the reaction of $\bullet\text{OH}$ radical with aromatic molecules in water has been established, for the first time, using time-resolved resonance Raman spectroscopy as a diagnostic tool and *p*-dimethoxybenzene as a model system. In the currently accepted mechanism, the cation radical is produced by $\bullet\text{OH}$ addition to the ring, followed by loss of OH^- . The present work demonstrates that this process competes with direct electron transfer. A generalized reaction mechanism has been proposed in terms of potential energy diagrams to explain two-step formation of the cation radical. In this reaction mechanism, the electron-transfer component and the rate of OH^- elimination from the $\bullet\text{OH}$ adduct both depend on the ionization potential (IP) of the molecule. The cation radical yield by electron transfer increases from 6% in *p*-dimethoxybenzene to 30% in *p*-anisidine and 85% in *p*-phenylenediamine. For neutral molecules with IP > 8 eV, the $\bullet\text{OH}$ addition is the first step in the chemistry, and for IP < 7 eV, it is the electron transfer. In the intermediate IP range, both processes occur simultaneously.

Introduction

The oxidation of organic substrates by the $\bullet\text{OH}$ radical is one of the most widely studied reactions because of its central role in chemistry and biology, organic synthesis, photocatalysis in aqueous environments, wastewater treatment, and numerous other chemical processes.^{1–10} The reaction is used to prepare radical intermediates in aqueous medium, to investigate their structure and reactivity by ESR and time-resolved Raman spectroscopy.^{9,11} However, the fundamental question of whether

the reaction involves an electron transfer (ET) component, and what mechanistic implications that would have for the early chemical events, has never been answered. In the commonly held reaction mechanism, the $\bullet\text{OH}$ radical reacts with aromatic molecules by addition to the ring.^{2–9} This behavior contrasts with the highly oxidizing nature of the $\bullet\text{OH}$ radical ($E^\circ(\bullet\text{OH}/\text{OH}^-) = 1.9 \text{ V}$)¹² that should generally favor electron transfer. The adduct (hydroxycyclohexadienyl) radicals undergo loss of OH^- by reaction with H^+ and/or water to form the cation radical (adduct-mediated electron transfer; AMET). The ET component in the reaction is difficult to recognize, and can be easily confused with AMET, for the following reasons: (1) Experimentally, a clear resolution cannot be made between the ET and AMET processes, unless the $\bullet\text{OH}$ addition (diffusion-controlled) and OH^- elimination occur at drastically different time scales. Obviously, the H^+ -catalyzed OH^- loss (generally diffusion controlled) must be avoided by making measurements in basic solutions. (2) The $\bullet\text{OH}$ adducts at the different ring sites decay at different rates, and not necessarily into the cation radical. Complications arise due to the presence of several transient species, with overlapping absorption, making identification and kinetic monitoring of the individual species quite difficult. To establish the ET component in the reaction, it is extremely important to select model systems in which the number of possible $\bullet\text{OH}$ adducts is small, and to use a structure-sensitive technique, such as time-resolved resonance Raman spectroscopy, for transient identification and kinetic monitoring.

[†] The research described herein was supported by the Office of Basic Energy Sciences, Department of Energy. This is Document No. NDRL-4044 from the Notre Dame Radiation Laboratory.

(1) See, *Biweekly List of Papers on Radiation Chemistry and Photochemistry*, published by the NDRL Data Center, Radiation Laboratory, University of Notre Dame, Notre Dame, IN. Farahataziz; Ross, A. B. *Selected Specific Rates of Reactions of Transients from Water in Aqueous Solution*, NSRDS–NBS 59; US Department of Commerce, 1977.

(2) Sonntag, C. v. *The Chemical Basis of Radiation Biology*; Taylor and Francis: New York, 1987.

(3) Tripathi, G. N. R.; Yu, S. J. *J. Am. Chem. Soc.* **1996**, *118*, 2235 and references therein.

(4) Viera, A. J. S. C.; Candeias, L. P.; Steenken, S. J. *Chim. Phys.* **1993**, *90*, 881. Viera, A. J. S. C.; Steenken, S. J. *Am. Chem. Soc.* **1990**, *112*, 6918; **1989**, *109*, 1987. Wu, Z.; Ahmad, R.; Armstrong, D. A. *Int. J. Radiat. Phys. Chem.* **1984**, *23*, 251. Elliot, A. J.; McEachern, R. J.; Armstrong, D. A. *J. Phys. Chem.* **1981**, *85*, 68. Clement, J. R.; Lin, W. S.; Armstrong, D. A. *Radiat. Res.* **1977**, *72*, 427.

(5) Neta, P. *Adv. Phys. Org. Chem.* **1976**, *12*, 2. Hapiot, P.; Pinson, J.; Francesch, C.; Mhamdi, F.; Rolando, C.; Neta, P. *J. Phys. Chem.* **1994**, *98*, 2641. Neta, P.; Madhavan, V.; Zemel, H.; Fessenden, R. W. *J. Am. Chem. Soc.* **1977**, *99*, 163. Neta, P.; Fessenden, R. W. *J. Phys. Chem.* **1974**, *78*, 523.

(6) Steenken, S. *Top. Curr. Chem.* **1996**, *177*, 125. Steenken, S. *J. Chem. Soc., Faraday Trans. 1* **1987**, *83*, 113 and references therein.

(7) Jagannadham, V.; Steenken, S. *J. Am. Chem. Soc.* **1985**, *107*, 6818. Jagannadham, V.; Steenken, S. *J. Am. Chem. Soc.* **1984**, *106*, 6542. Hazra, D. K.; Steenken, S. *J. Am. Chem. Soc.* **1983**, *105*, 4380. Steenken, S.; Raghavan, N. V. *J. Phys. Chem.* **1979**, *83*, 3101.

(8) Walling, C.; Camaioni, D. M.; Kim, S. S. *J. Am. Chem. Soc.* **1978**, *100*, 1603. Walling, C.; Camaioni, D. M. *J. Am. Chem. Soc.* **1975**, *97*, 1603. Walling, C.; Johnson, R. A. *J. Am. Chem. Soc.* **1975**, *97*, 363 and references therein.

(9) Nonhebel, D. C.; Walton, J. C. *Free-radical Chemistry: Structure and Mechanism*; Cambridge University Press: New York, 1974.

(10) Bard, A. J.; Fox, M. A. *Acc. Chem. Res.* **1995**, *28*, 141. Fox, M. A. *Sol. Energy Mater.* **1995**, *38*, 381. Fox, M. A. In *Photocatalytic Purification and Treatment of Water and Air*; Ollis, D. F., Al-Ekabi, Eds.; Elsevier: Amsterdam, 1995, Vol. 3, p 163. Goldstein, S.; Czapski, G.; Rabani, J. *J. Phys. Chem.* **1994**, *98*, 6586. Brandys, M.; Sassoon, R. E.; Rabani, J. *J. Phys. Chem.* **1987**, *91*, 953. Jaeger, C. D.; Bard, A. J. *Phys. Chem.* **1979**, *83*, 3146. Draper, R. B.; Fox, M. A.; Pelizzetti, E.; Serpone, N. *J. Phys. Chem.* **1989**, *93*, 1938 and references therein.

(11) Tripathi, G. N. R. In *Advances in Spectroscopy, Vol. 18, Time-resolved Spectroscopy*; Clark, R. J. H., Hester, R. E., Eds.; John Wiley & Sons: New York, 1989; pp 157–218.

(12) Wardman, P. *J. Phys. Chem. Ref. Data* **1989**, *18*, 1637.

In para disubstituted benzenes, there are four equivalent ring sites and two equivalent ipso positions. Therefore, only two types of $\bullet\text{OH}$ adduct and, at most, four transients, including radical products of the $\bullet\text{OH}$ adducts, are possible in the AMET mechanism. Therefore, they are expected to be satisfactory model systems. The radicals derived from benzene derivatives in water generally have strong absorption in the near-UV and visible regions, which is essential for high detection sensitivity in resonance Raman methods.¹¹ In the model systems, the radicals produced initially by the ET as well as the AMET mechanism must be observable, so that it can be shown kinetically that the adduct radical is not the precursor of the cation radical. Unfortunately, not many para disubstituted benzenes satisfy this criterion. To illustrate this point, we refer to a recent examination of the $\bullet\text{OH}$ oxidation of *p*-diaminobenzene (*p*-phenylenediamine) in basic aqueous solutions by time-resolved resonance Raman spectroscopy.¹³ In this case, the $\bullet\text{OH}$ adduct at the ipso position may produce the *p*-aminophenoxy radical by NH_3 elimination. However, this product radical was not observed. The initial transient absorption spectrum that was attributed to the $\bullet\text{OH}$ adduct in the literature,¹⁴ in support of AMET, was found to be that of the cation radical.¹³ The cation radical forms in two steps, with the major fraction ($85 \pm 5\%$) at a diffusion-controlled rate, and the minor ($15 \pm 5\%$) with a period of ~ 50 ns. Thus, ET appears to be the dominant reaction pathway in this aromatic diamine. However, the adduct radical, expected to appear simultaneously with 85% of the cation radicals (ET) and produce 15% of the cation radicals on decay (AMET), absorbs too weakly to be identified.¹³ While the cation radical formation in two steps cannot be explained by AMET alone, the production of the $\bullet\text{OH}$ adduct and cation radicals at the same rate would be straightforward and convincing experimental evidence for the existence of ET.¹⁵

In our search for appropriate model systems, we find that the existence of an ET component can be unambiguously demonstrated in the reaction of $\bullet\text{OH}$ radical with *p*-dimethoxybenzene (DMB) in water. This molecule does not undergo structural modifications due to protonation/deprotonation in moderately acidic and basic solutions, a problem associated with most hydroxy and amino compounds. Its radical cation may react with base,¹⁶ but even at a diffusion-controlled rate ($\sim 10^{10} \text{ M}^{-1} \text{ s}^{-1}$) of the reaction, a significant decrease in the cation radical yield on the submicrosecond time scale can occur only at $\text{pH} > 10$. The Raman evidence of a fast and a slow component in the formation kinetics of cation radical in the $\bullet\text{OH}$ oxidation of *p*-methoxyaniline (*p*-anisidine) is also presented. It is shown that the AMET mechanism for the $\bullet\text{OH}$ oxidation is exclusive only for aromatic molecules with ionization potentials greater than 8 eV. For molecules with lower ionization potential, competition between ET and AMET mechanisms must be considered.

Experimental Procedure

The $\bullet\text{OH}$ radical was produced by pulse radiolysis of N_2O -saturated water. The radiolysis of oxygen-free water produces e_{aq}^- (2.6), $\bullet\text{OH}$ (2.7), and H^\bullet (0.6) radicals (numbers in parentheses are *G* values, i.e.,

(13) Sun, Q.; Tripathi, G. N. R.; Schuler, R. H. *J. Phys. Chem.* **1990**, *94*, 2216.

(14) Rao, P. S.; Hayon, E. *J. Phys. Chem.* **1975**, *79*, 1063.

(15) The observed rates of adduct and cation radicals should be the same and equal to the rate of $\bullet\text{OH}$ encounter with the molecule (diffusion-controlled), if they are produced simultaneously. In this work, we are concerned only with the observed rates. The second-order rate constant for a product radical can be derived by multiplying the rate constant for the $\bullet\text{OH}$ encounter with the measured yield of the radical.

(16) Tripathi, G. N. R. *Chem. Phys. Lett.* **1992**, *199*, 409. Holcman, J.; Sehested, K. *J. Phys. Chem.* **1976**, *80*, 1642.

yields of radicals per 100 eV of energy absorbed) on the 100 ns time scale.¹⁷ The e_{aq}^- reacts with N_2O , converting into the $\bullet\text{OH}$ radical in less than 5 ns. The H^\bullet radical is a minor product of radiolysis that reacts with aromatic molecules by addition, but does not form the cation radical.¹⁷ The oxidizing species $\text{SO}_4^{\bullet-}$ was prepared by the reaction of e_{aq}^- with persulfate dianion ($e_{\text{aq}}^- + \text{S}_2\text{O}_8^{2-} \rightarrow \text{SO}_4^{2-} + \text{SO}_4^{\bullet-}$) in N_2 -saturated solutions.¹⁸ In that case, the $\bullet\text{OH}$ radical was scavenged by adding an excess of *tert*-butyl alcohol (*t*-BuOH) in solution. The radiation yield of $\text{SO}_4^{\bullet-}$ was taken to be half the yield of the $\bullet\text{OH}$ radical in N_2O -saturated water. The $\text{SO}_4^{\bullet-}$ radical generally reacts with organic substrates by electron transfer.¹⁸ Comparison of the initial radical cation yield in the reaction of $\bullet\text{OH}$ radical with that of $\text{SO}_4^{\bullet-}$, after compensation for the radiation yields, gives the fraction of the $\bullet\text{OH}$ radical involved in electron transfer. If this fraction is small, identification of the cation radical, estimation of its yield, and determination of its growth kinetics are almost impossible by the optical absorption method due to overlapping absorption by other radicals present in much larger concentrations. Therefore, the time-resolved resonance Raman method was used for detection.¹¹

The pulse radiolysis time-resolved Raman spectroscopic technique used in this Laboratory for the study of short-lived chemical intermediates in solution has been described in detail elsewhere.^{11,19} In brief, a Van de Graaff accelerator is used to generate 2 MeV, 100 ns electron pulses for radiolysis. A tunable excimer laser pulse pumped dye laser (10 ns) system is used to probe Raman scattering, and an optical multichannel analyzer (OMA) accompanied by an intensified gated (20 ns) diode array is used for detection. The accelerator and laser are operated at a repetition rate of 7.5 Hz, which allows efficient signal averaging. Raman band positions are measured with reference to the known Raman bands of common solvents such as ethanol, and are accurate to within $\pm 2 \text{ cm}^{-1}$ for sharp bands and $\pm 5 \text{ cm}^{-1}$ for broad and shoulder bands.

The initial $\bullet\text{OH}$ concentration in our experimental conditions was $\sim 10^{-5} \text{ M}$. The Raman spectra were generally excited off-resonance and the scattering center was carefully positioned close to the bottom of the Raman cell (within 0.4 mm), to minimize attenuation of the probe laser and scattered signals. The experiments were mostly performed in neutral and basic solutions, so that H^+ -catalyzed OH^- loss from the adduct radicals would not contribute to the cation radical signals.

Results and Discussion

The optical absorption spectra and rate parameters available from an earlier study on the $\bullet\text{OH}$ reaction with *p*-dimethoxybenzene²⁰ were used to define the chemical conditions under which cation radical formation by electron transfer (ET) could be distinguished from that by adduct-mediated electron transfer (AMET). *p*-Dimethoxybenzene is not very soluble in water, and only $3 \times 10^{-4} \text{ M}$ of it could be dissolved in solution. The reaction occurs with a rate constant of $7 \times 10^9 \text{ M}^{-1} \text{ s}^{-1}$, equivalent to a rate of $2.1 \times 10^6 \text{ s}^{-1}$ for the substrate concentration used in the present work. Initially, a transient absorption with λ_{max} at 300 nm, attributed to the $\bullet\text{OH}$ adduct (DMB- OH^\bullet), appears. In acidic solutions, the adduct radical decays, by the reaction with H^+ , at a rate constant of $2 \times 10^8 \text{ M}^{-1} \text{ s}^{-1}$, into a transient species with λ_{max} in the 460 nm region, assigned to the cation radical (DMB $^{\bullet+}$). The bimolecular reactions of the $\bullet\text{OH}$ adduct occur at a rate constant ($2k$) of $\sim 10^9 \text{ M}^{-1} \text{ s}^{-1}$, corresponding to an initial decay rate of $\sim 5 \times 10^3 \text{ s}^{-1}$ for the radical concentration of $\sim 5 \times 10^{-6} \text{ M}^{-1}$, used

(17) Buxton, G. V.; Greenstock, C. L.; Helman, W. P.; Ross, A. B. *J. Phys. Chem. Ref. Data* **1988**, *17*, 513.

(18) Neta, P.; Huie, R. E.; Ross, A. B. *J. Phys. Chem. Ref. Data* **1988**, *17*, 1027.

(19) Tripathi, G. N. R. In *Multichannel Image Detectors II*; Talmi, Y., Ed.; ACS Symp. Ser. No. 236 American Chemical Society, Washington, DC, 1983; p 171.

(20) O'Neill, P.; Steenken, S.; Schulte-Frohlinde, D. *J. Phys. Chem.* **1975**, *79*, 2773.

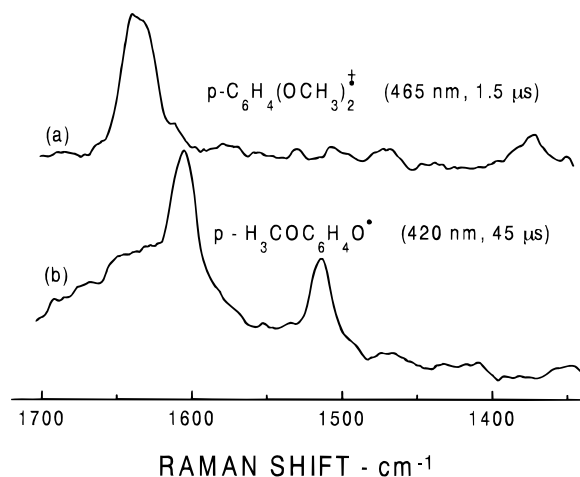


Figure 1. Transient Raman spectra obtained by excitation at (a) 465 nm, 1.5 μs after the electron pulse, and (b) 420 nm, 45 μs after the electron pulse on pulse radiolysis of an N_2O -saturated aqueous solution of *p*-dimethoxybenzene (pH 7, phosphate buffer).

in the optical absorption work.²⁰ At pH > 6, the rate of cation radical formation by the reaction of adduct radicals with H^+ , i.e., $< 2 \times 10^2 \text{ s}^{-1}$, is much slower than the bimolecular reaction rate ($\sim 5 \times 10^3 \text{ s}^{-1}$). The formation of the cation radical by water-catalyzed loss of OH^- from DMB-OH^* was also not seen. Therefore, the rate was estimated to be $< 10^3 \text{ s}^{-1}$.²⁰ Thus, one cannot observe the cation radical, on the microsecond and shorter time scale, by the AMET process, at pH > 6. In basis solutions, $\text{DMB}^{+\bullet}$ may react with OH^- .¹⁶ However, even if the reaction is diffusion controlled, its rate can be comparable to or faster than the rate of $\bullet\text{OH}$ reaction with DMB ($2.1 \times 10^6 \text{ s}^{-1}$) only at pH > 10. Therefore, if $\text{DMB}^{+\bullet}$ is produced in the reaction, it should be observable, with the yield decreasing rapidly as pH exceeds 10.

From the above analysis, it is clear that if there is an electron-transfer component in the reaction, the most suitable pH range for its evaluation would be between 7 and 9.

Raman Observation of the $\text{DMB}^{+\bullet}$ Cation Radical. N_2O -saturated aqueous solutions containing $3 \times 10^{-4} \text{ M}$ DMB at pH 7 ± 0.2 (phosphate buffer) were subjected to pulse radiolysis. The formation kinetics of $\text{DMB}^{+\bullet}$ was monitored by time-resolved resonance Raman spectroscopy with an excitation wavelength of 465 nm (λ_{max} of $\text{DMB}^{+\bullet}$ at 460 nm). Contrary to the expectations for the AMET mechanism, we observe a transient Raman spectrum of $\text{DMB}^{+\bullet}$, with prominent bands at ~ 1640 and $\sim 1375 \text{ cm}^{-1}$ (Figure 1a). Identification of the spectrum as that of $\text{DMB}^{+\bullet}$ follows directly from comparison with spectra obtained in chemical oxidation reactions.²¹ The Raman signals evolved on the 100 ns time scale (Figure 2). The growth half-period was measured as 300 (± 50) ns, which corresponds to a rate constant of $7.7 (\pm 1.3) \times 10^9 \text{ M}^{-1} \text{ s}^{-1}$ ($6 \times 10^9 \text{ M}^{-1} \text{ s}^{-1}$ by fitting the data with first-order kinetics; see Figure 2). This rate constant matches well, within experimental uncertainty, with the rate constant for the formation of $\bullet\text{OH}$ adduct to DMB ($7 \times 10^9 \text{ M}^{-1} \text{ s}^{-1}$), available in the literature.²⁰ The rate of $\text{DMB}^{+\bullet}$ production was found to be independent of the buffer concentration, but depended linearly on the DMB concentration in solution. When an excess of *t*-BuOH was added to the solution, to scavenge $\bullet\text{OH}$ radicals, the $\text{DMB}^{+\bullet}$ Raman signals disappeared. The transient Raman signals of $\text{DMB}^{+\bullet}$ were observable even at pH 11, 100 ns after the pulse,

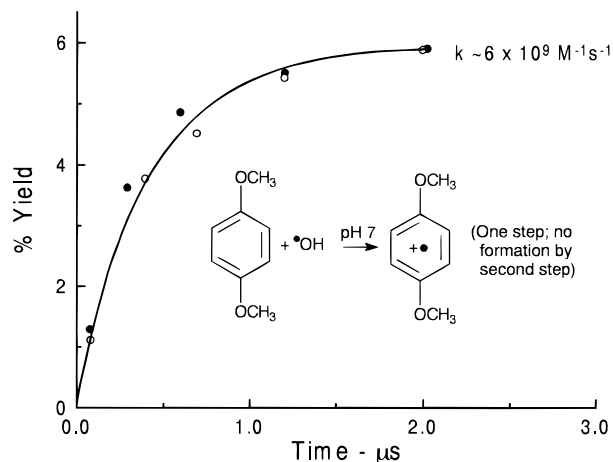


Figure 2. Formation kinetics of the *p*-dimethoxybenzene cation radical ($\text{DMB}^{+\bullet}$; 6% yield) on $\bullet\text{OH}$ oxidation of *p*-dimethoxybenzene ($3 \times 10^{-4} \text{ M}$, pH 7, N_2O saturated). The solid circles (●) show the formation kinetics of $\text{DMB}^{+\bullet}$ produced by $\text{SO}_4^{\bullet-}$ oxidation (100% yield). The reaction rates of $\bullet\text{OH}$ and $\text{SO}_4^{\bullet-}$ are comparable.

without phosphate buffer in solution, but with reduced intensity, as expected due to the rapid loss of cation radical by reaction with OH^- .¹⁶

The straightforward kinetic Raman observation of $\text{DMB}^{+\bullet}$, in the $\text{DMB} + \bullet\text{OH}$ reaction in water, at a rate comparable to that of $\bullet\text{OH}$ adduct, provides unambiguous experimental evidence of the electron-transfer component in the reaction.¹⁵ As discussed earlier, the formation of $\text{DMB}^{+\bullet}$ on the 100 ns time scale at neutral pH cannot be explained by the reaction of DMB-OH^* with H^+ , as this process, even at a diffusion-controlled rate, would require 100 ms or longer time. The water-induced dissociation of the adducts into the radical cation must be ruled out, as the process is too slow ($k < 10^3 \text{ s}^{-1}$) to contribute on the 100 ns time scale. The reaction of DMB-OH^* with buffer cannot be a contributing factor, as (1) buffer concentration (1 to 10 mM) had no effect on the cation radical yield and (2) weak cation radical signals were observed even at pH 11, 100 ns after the electron pulse, without phosphate buffer in solution. Most importantly, any imaginable reaction of the $\bullet\text{OH}$ adduct that can give cation radical (AMET) on the 100 ns time scale will lead to its complete disappearance within a few microseconds, and in no case will the cation radical evolve at the same rate as the $\bullet\text{OH}$ adduct.

The yield of $\text{DMB}^{+\bullet}$ produced by electron transfer (ET) from DMB to $\bullet\text{OH}$ was determined by comparison with the yield (Raman signal intensity) obtained when DMB was oxidized by radiolytically produced $\text{SO}_4^{\bullet-}$ in a N_2 -saturated solution ($\text{DMB} + \text{SO}_4^{\bullet-} \rightarrow \text{DMB}^{+\bullet} + \text{SO}_4^{2-}$). The spectra were scaled for the radiation yields of $\bullet\text{OH}$ and $\text{SO}_4^{\bullet-}$ radicals. We find that the $\text{DMB}^{+\bullet}$ cation radical yield by ET is only $6(\pm 2)\%$. Therefore, it is not surprising that the cation radical formation by ET was not detected by transient absorption and that only the adduct absorption which does not decay even on the 100 μs time scale, was observed.²⁰ The observed rate for the 6% $\text{DMB}^{+\bullet}$ production in the $\bullet\text{OH}$ reaction is compared, in Figure 2, with the formation rate for 100% $\text{DMB}^{+\bullet}$ in the $\text{SO}_4^{\bullet-}$ oxidation (electron transfer),²⁰ with $3 \times 10^{-4} \text{ M}$ of DMB in solution at pH 7. It can be seen that both rates are diffusion controlled and comparable. Thus, we have conclusive experimental evidence that $\bullet\text{OH}$ oxidation can involve electron transfer. In the $\bullet\text{OH}$ oxidation of *p*-phenylenediamine where the adduct absorption is not observed, the yield of the cation radical (85%) produced at a diffusion-controlled rate can be safely attributed

(21) Ernstbrunner, E. E.; Girling, R. B.; Grossman, W. E. L.; Hester, R. E. *J. Chem. Soc., Perkin Trans. 2* **1978**, 177.

to ET, and the remaining 15% (~50 ns) to AMET.¹³ In this respect, *p*-dimethoxybenzene and *p*-phenylenediamine are deemed to represent two extreme cases. It would be logical to expect *p*-methoxyaniline (*p*-anisidine) to display an intermediate behavior. We will discuss, later on, the cation radical formation on $\bullet\text{OH}$ oxidation of *p*-anisidine in water.

Raman Observation of the *p*-Methoxyphenoxy Radical.

We have also observed formation of the *p*-methoxyphenoxy radical (MPhO \bullet) on the $\bullet\text{OH}$ oxidation of DMB. The Raman excitation in this case was at 420 nm (λ_{max} of MPhO \bullet at 415 nm).¹¹ This transient is formed at a slower rate than the DMB $^{+\bullet}$ cation radical. The spectrum of the species recorded 45 μs after the electron pulse, after subtraction of the DMB $^{+\bullet}$ Raman signals, is shown in Figure 1b. The Raman signals (bands at 1609 and 1518 cm^{-1})^{11,22} of this transient disappear on addition of *t*-BuOH to the solution. No Raman signal is observed on radiolysis of solutions containing 3×10^{-4} M DMB and 0.1 M NaN_3 ($\text{N}_3\bullet$ radical oxidizes *p*-methoxyphenol but not DMB), showing that the MPhO \bullet radical originates from DMB and not from an impurity of *p*-methoxyphenol in the sample. The yield of MPhO \bullet radical in the reaction of $\bullet\text{OH}$ with DMB was determined by comparison with the yield observed in the reaction of $\text{N}_3\bullet$ radical with *p*-methoxyphenol in basic aqueous solutions.^{11,22} The $\text{N}_3\bullet$ radical is produced by the electron-transfer reaction of $\bullet\text{OH}$ radical with N_3^- (0.1 M). Therefore, the radiation yield was taken to be the same as that of $\bullet\text{OH}$. We find that $12(\pm 2)\%$ of the $\bullet\text{OH}$ radicals are consumed in the formation of MPhO \bullet , in the $\bullet\text{OH}$ oxidation of DMB in near neutral solutions. Since this radical is formed at a slower rate than DMB $^{+\bullet}$ (microsecond time scale), it cannot be considered the initial reaction product. Its logical precursor is the $\bullet\text{OH}$ adduct at the ipso position which converts into phenoxy radical by methanol elimination.²³ It appears that about 94% of the $\bullet\text{OH}$ radicals produced in the radiolysis of water add to the DMB ring, in the ratio of 1:8 for ipso to nonipso positions.

In contrast to *p*-dimethoxybenzene, the *p*-aminophenoxy radical was not observed in the $\bullet\text{OH}$ oxidation of *p*-phenylenediamine. This is readily understandable, as only a small fraction (15%) of the $\bullet\text{OH}$ radicals add to the ring.¹³

The $\bullet\text{OH}$ Oxidation of *p*-Anisidine. As pointed out earlier, *p*-dimethoxybenzene and *p*-phenylenediamine represent two extreme situations with respect to ET vs AMET mechanisms, and *p*-anisidine is a logical intermediate case. However, the number of $\bullet\text{OH}$ adducts and their transient radical products likely to be produced doubles due to molecular asymmetry. We focus here only on the growth kinetics of the cation radical, monitored at its characteristic resonance Raman bands (1624, 1519, and 1400 cm^{-1}).²⁴ An N_2O -saturated aqueous solution containing 2×10^{-3} M *p*-methoxyaniline at pH 7 (substrate acts as buffer) was subjected to pulse radiolysis. The temporal evolution of the Raman bands (excitation in resonance with λ_{max} of the cation radical at 445 nm) is depicted in Figure 3. It is clearly evident from Figure 3 that the cation radical is formed in two steps. The initial step is responsible for about 38% of the cation radicals produced in the reaction. Both steps combined account for 80% of the $\bullet\text{OH}$ radicals (by comparison with the signals observed by $\text{N}_3\bullet$ oxidation). About 10% *p*-aminophenoxy radical¹¹ is also produced in the reaction, but Raman signals of

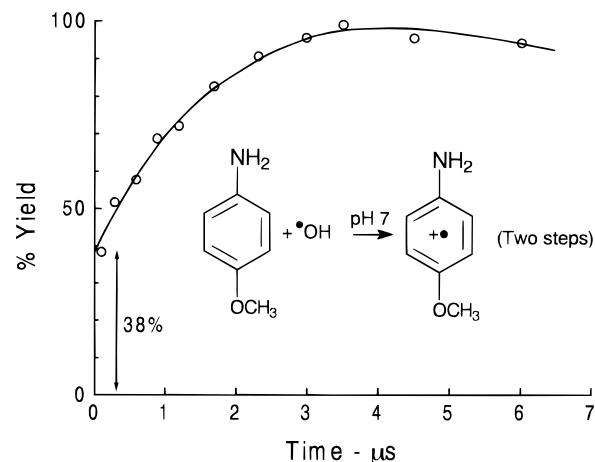
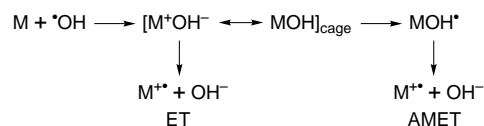


Figure 3. Formation kinetics of the cation radical produced on $\bullet\text{OH}$ oxidation of *p*-anisidine (2×10^{-3} M, pH 7, N_2O saturated) in water.

p-methoxyphenoxy radical were not detected. We estimate that at least 30% of the $\bullet\text{OH}$ radicals produce the cation radical by the first step, a yield approximately five times that in *p*-dimethoxybenzene (6%) and about one-third that in *p*-phenylenediamine (85%).²⁵ At pH >7, the rate of cation radical formation by the second step was found to be less than 10^3 s^{-1} in *p*-dimethoxybenzene and $\sim 2 \times 10^7 \text{ s}^{-1}$ in *p*-phenylenediamine.¹³ In *p*-anisidine, this rate is about $9 \times 10^5 \text{ s}^{-1}$. Thus, with an increase in the ET component in the reaction, the rate of cation radical formation by AMET also increases. This is an important observation that will be explained by the reaction mechanism that we discuss in the following subsection.

Reaction Mechanism

The following reaction scheme, inclusive of the ET and AMET steps, accounts for the experimental observations made to date.



The two-step formation of the cation radical ($\text{M}^{+\bullet}$) in the above reaction scheme, if analyzed in terms of potential energy diagrams, provides a clear insight into the early chemical events and leads to valuable guidance for identifying the chemical systems in which electron transfer can be observed.

Let us consider, for the sake of simplicity, that M and $\bullet\text{OH}$ act as atomic species that bond on encounter. The interaction potential at various interatomic distances can be totally, or in part, covalent (MOH) or ionic (M^+OH^-), depending on the relative energies of the corresponding electronic configurations, with respect to the energy of $\text{M} + \bullet\text{OH}$ (Figure 4). In the covalent configuration MOH, the C–OH bond (typically 1.5 Å)²⁶ can form due to orbital overlap between an unpaired electron on O and a ring $\text{p}(\pi)$ -electron, at the expense of the ring CC (π) bonds. The energy difference between the CO (σ)

(22) Tripathi, G. N. R.; Schuler, R. H. *J. Phys. Chem.* **1987**, *91*, 5881.

(23) Raghavan, N. V.; Steenken, S. *J. Am. Chem. Soc.* **1980**, *102*, 3495. Steenken, S.; O'Neill, P. *J. Phys. Chem.* **1977**, *81*, 505. O'Neill, P.; Schulte-Frohlinde, D.; Steenken, S. *J. Chem. Soc., Faraday Discuss.* **1977**, *63*, 141. O'Neill, P.; Steenken, S. *Ber. Bunsen-Ges. Phys. Chem.* **1977**, *81*, 550.

(24) (24) Sun, Q.; Tripathi, G. N. R.; Schuler, R. H. *J. Phys. Chem.* **1990**, *94*, 6273.

(25) Because of molecular asymmetry, *p*-anisidine is not an acceptable model for establishing ET, as one can postulate an extremely short-lived adduct precursor for the diffusion-controlled component (38%) in the cation radical formation. Experimentally, only one $\bullet\text{OH}$ adduct with absorption in the 330 nm region is seen which decays at a rate of $9 \times 10^5 \text{ s}^{-1}$. The data on *p*-anisidine should be viewed in the light of results on *p*-dimethoxybenzene and *p*-phenylenediamine.

(26) Pauling, L. *The Nature of the Chemical Bond*; Cornell University Press: Ithaca, New York, 1960.

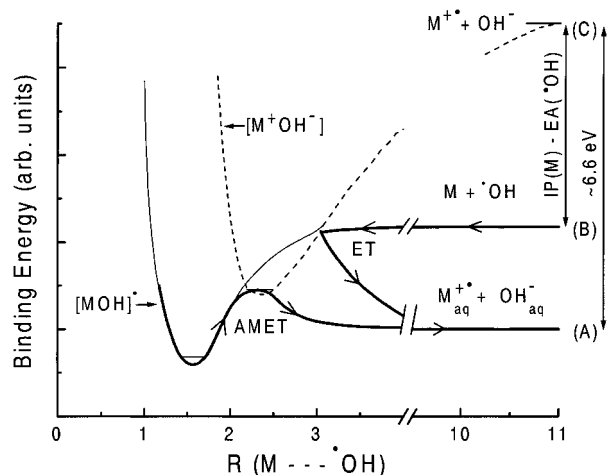


Figure 4. Direct electron transfer (ET) and $\bullet\text{OH}$ adduct mediated electron transfer (AMET) processes explained by qualitative potential energy diagrams (see text).

and CC (π) bonds is known to be small (~ 20 kcal/mol or 0.87 eV).²⁶ Therefore, the MOH potential well cannot be very deep (< 1 eV), irrespective of the nature of M. The difference between the ionization potential (IP in eV) of M and the electron affinity (EA) of $\bullet\text{OH}$ (1.83 eV)²⁷ gives the asymptotic energy difference between $\text{M}^{+\bullet} + \text{OH}^-$ and $\text{M} + \bullet\text{OH}$ (Figure 4B,C). If the electrostatic binding energy of $\text{M}^{+\bullet}\text{OH}^-$ becomes greater than $\text{IP}(\text{M}) - \text{EA}(\bullet\text{OH})$, the $\bullet\text{OH} + \text{M}$ encounter can lead to the ionic ($\text{M}^{+\bullet}\text{OH}^-$) configuration (Figure 4B). It should be noted that the Coulombic binding energy of oppositely charged centers, separated by $< 2.5 \text{ \AA}$, is greater than 5 eV, and $\text{IP}(\text{M}) \sim 7$ eV is not uncommon in organic molecules.²⁸ The Coulombic potential energy curves, in general, are steeper than the covalent potential energy curves, except for M and $\bullet\text{OH}$ separations close to the MOH bonding distances.²⁶ In nonpolar solvents, the ionic configuration, $\text{M}^{+\bullet}\text{OH}^-$, will eventually terminate into the covalent configuration, on dissipation of the excess energy as thermal energy.^{29,30} However, if the $\text{M}^{+\bullet}\text{OH}^-$ dipole is created in a polar solvent like water (dielectric constant, ϵ , ~ 80), the ionic components can solvate and separate rapidly (< 100 fs)^{29,30} (Figure 4A,B). Experimentally, $\text{M}^{+\bullet}$ will be observed to appear at the rate of $\bullet\text{OH}$ encounter with M, i.e., at a diffusion-controlled rate.

The hydration free energies (ΔG°) of OH^- and benzene-size cations are estimated as -4 (91 kcal mol⁻¹)³¹ and -2.6 eV (60 ± 8 kcal mol⁻¹),²⁷ respectively, which gives the free energy difference between $\text{M}^{+\bullet} + \text{OH}^-$ and $\text{M}_{\text{aq}}^{+\bullet} + \text{OH}_{\text{aq}}^-$ as 6.6 eV (Figure 4A,C). If the hydration energies of neutral $\bullet\text{OH}$ (-0.2 eV) and M (-0.1 eV)²⁷ are ignored, the free energy difference between $\text{M}_{\text{aq}} + \bullet\text{OH}_{\text{aq}}$ and $\text{M}_{\text{aq}}^{+\bullet} + \text{OH}_{\text{aq}}^-$ comes

(27) Pearson, R. G. *J. Am. Chem. Soc.* **1986**, *108*, 6109.

(28) Rosenstock, H. M.; Draxl, K.; Steiner, B. W.; Herron, J. T. *J. Phys. Chem. Ref. Data* **1977**, *6*, Suppl. 1.

(29) For solvation time of medium size molecular ions in nonpolar solvents (55–90 ps), see: Lin, Y.; Jonah, C. *J. Phys. Chem.* **1992**, *96*, 10119. The solvation time decreases by more than two orders of magnitude in acetonitrile (~ 0.3 ps). The trends indicate that the combined rate of $\text{M}^{+\bullet}$ and OH^- hydration should be much faster. Professor Barbara (private discussion) suggests a time scale of < 50 fs for a major portion of the hydration energy (~ 4 eV) of OH^- .

(30) For vibrational relaxation time (a few picoseconds), see: Harris, A. L.; Brown, J. K.; Harris, C. B. *Annu. Rev. Phys. Chem.* **1988**, *39*, 341. Benjamin, I.; Barbara, P. F.; Bradley, J. G.; Hynes, J. R. *J. Phys. Chem.* **1995**, *99*, 7557. Walhout, P. K.; Alfano, J. C.; Khalid, A. M. T.; Barbara, P. F. *J. Phys. Chem.* **1995**, *99*, 7568. Dieter, P. J. In *Radiationless Processes*; Fong, F. K., Ed.; Springer-Verlag: New York, 1976; p 169.

(31) Friedman, H. L.; Krishnan, C. V. In *Water: A Comprehensive Treatise*; Franks, F., Ed.; Plenum Press: New York, 1973; Vol. 3.

out to be $8.4 \text{ eV} - \text{IP}(\text{M})$ (EA of $\bullet\text{OH}$ taken as 1.8 eV).²⁷ For $\text{IP}(\text{M}) > 8.4$ eV (back reaction faster than forward reaction), $\text{M}_{\text{aq}}^{+\bullet}$ will be difficult to observe in basic solutions, even if produced exclusively by ET. The free energy difference between $\text{M}_{\text{aq}} + \bullet\text{OH}_{\text{aq}}$ and $\text{M}_{\text{aq}}^{+\bullet} + \text{OH}_{\text{aq}}^-$ increases by 0.83 eV on OH^- protonation ($0.059 \times \text{p}K_{\text{a}}$ of water). Therefore, for $\text{IP}(\text{M}) > 9.2$ eV, $\text{M}_{\text{aq}}^{+\bullet}$ will be difficult to observe even in neutral and acidic aqueous solutions. The numerical values used here are very approximate. However, this simple thermodynamical analysis explains why the H^+ -catalyzed loss of OH^- from the $\bullet\text{OH}$ adducts of molecules with high $\text{IP}(\text{M})$, such as benzene, is not observed.⁶ The effect of $\text{IP}(\text{M})$ in converting the initial chemical step from $\bullet\text{OH}$ addition to electron transfer can be readily visualized by raising or lowering the ionic potential energy curve C in Figure 4.

While the above description of the reaction mechanism is illustrative, it is too simplistic, and of little quantitative significance in predicting the ET component. In particular, there can be several isomers of MOH and the $\text{M}^{+\bullet}\text{OH}^-$ configurations, each contributing to the overall reaction process. Fortunately, the molecular systems for which the ET components are discussed here represent low (6%), middle (30%), and high (85%) points of $\text{IP}(\text{M})$ dependence. This makes it possible to derive some extremely important conclusions, without recourse to the details of the reaction model. For *p*-dimethoxybenzene, $\text{IP}(\text{M}) = 7.8$ eV.²⁸ Therefore, it can be safely assumed that for $\text{IP}(\text{M}) > 8$ eV, which is the case for many benzene derivatives, the $\bullet\text{OH}$ reaction will lead to adduct formation only. On the other hand, for *p*-phenylenediamine, $\text{IP}(\text{M}) = 7.1$ eV,²⁸ which implies that for $\text{IP}(\text{M}) < 7$ eV, the reaction must be considered an electron-transfer reaction.

The property of the $\bullet\text{OH}$ adducts to undergo loss of OH^- in water (AMET) can also be understood in terms of $\text{IP}(\text{M})$.³² The covalent configuration MOH is unlikely to undergo ionic dissociation under the influence of solvent dielectric field. However, the ionic configuration $\text{M}^{+\bullet}\text{OH}^-$ can be thermally accessed from the adduct (MOH) ground state (Figure 4). The adduct radical will dissociate into solvated fragments $\text{M}^{+\bullet}$ and OH^- , at a rate of $k_{\text{d}} \exp(-\Delta E/RT)$, where k_{d} is the solvent-induced rate of dissociation in the $\text{M}^{+\bullet}\text{OH}^-$ configuration, and ΔE is the energy gap between MOH and $\text{M}^{+\bullet}\text{OH}^-$. This situation is very similar to the thermal dissociation of structurally stable radicals in solution for which a two-state model has been proposed recently.³ As is evident from the energy diagrams in Figure 4, ΔE depends on $\text{IP}(\text{M})$. The ET is high for low $\text{IP}(\text{M})$, which also means low ΔE , and, therefore, a faster rate of OH^- elimination in AMET. Thus, both steps of cation radical formation are intimately related.

Conclusion

A direct electron transfer path in the hydroxyl radical reaction with aromatic molecules in water has been experimentally demonstrated in selected model systems. This result has far-reaching consequences for understanding the early chemical events in one of the most widely studied reactions in chemistry. The extent of electron transfer is directly related to the ionization potential of the aromatic molecule. A potential energy model for the reaction, consistent with the observations, has been advanced.

It is not uncommon to see a small but fast component in the growth kinetics of cation radical in various systems, monitored

(32) Holcman, J.; Sehested, K. *Nukleonika* **1979**, *24*, 887.

by optical absorption.³³ The contribution is often ignored, or interpreted without supporting evidence. Structure-sensitive techniques, such as pulse radiolysis time-resolved Raman spectroscopy, are essential for probing the nature and origin of the individual components in the reaction. However, the knowledge that the hydroxyl radical does involve an electron transfer, and that this contribution depends on the ionization

(33) Qin, L.; Tripathi, G. N. R.; Schuler, R. H. *Z. Naturforsch. Teil A* **1985**, *40*, 1026 (a small ET component (4%) was noticed in the transient absorption study of the $\bullet\text{OH}$ oxidation of aniline (IP 7.7 eV) in water).

potential of the molecule in question, can be extremely valuable in interpreting the kinetic and spectral data obtained by the commonly used transient absorption method.

Acknowledgment. The author wishes to thank Dr. John Bentley and Professor Paul Barbara for illuminating discussions on the reaction mechanism and ionic solvation.

JA9800838